Intestinal serotonin and fluoxetine exposure modulate bacterial colonization in the gut

Thomas C. Fung [ID][1]*, Helen E. Vuong[1], Cristopher D. G. Luna[1], Geoffrey N. Pronovost[1], Antoniya A. Aleksandrova[2], Noah G. Riley[2], Anastasia Vavilina [ID][1], Julianne McGinn[1], Tomiko Rendon[1], Lucy R. Forrest [ID][2] and Elaine Y. Hsiao [ID][1]*

The gut microbiota regulates levels of serotonin (5-hydroxy-tryptamine (5-HT)) in the intestinal epithelium and lumen[1-5]. However, whether 5-HT plays a functional role in bacteria from the gut microbiota remains unknown. We demonstrate that elevating levels of intestinal lumenal 5-HT by oral supplementation or genetic deficiency in the host 5-HT transporter (SERT) increases the relative abundance of spore-forming members of the gut microbiota, which were previously reported to promote host 5-HT biosynthesis. Within this microbial community, we identify _Turicibacter sanguinis_ as a gut bacterium that expresses a neurotransmitter sodium symporter-related protein with sequence and structural homology to mammalian SERT. _T. sanguinis_ imports 5-HT through a mechanism that is inhibited by the selective 5-HT reuptake inhibitor fluoxetine. 5-HT reduces the expression of sporulation factors and membrane transporters in _T. sanguinis_, which is reversed by fluoxetine exposure. Treating _T. sanguinis_ with 5-HT or fluoxetine modulates its competitive colonization in the gastrointestinal tract of antibiotic-treated mice. In addition, fluoxetine reduces the membership of _T. sanguinis_ in the gut microbiota of conventionally colonized mice. Host association with _T. sanguinis_ alters intestinal expression of multiple gene pathways, including those important for lipid and steroid metabolism, with corresponding reductions in host systemic triglyceride levels and inguinal adipocyte size. Together, these findings support the notion that select bacteria indigenous to the gut microbiota signal bidirectionally with the host serotonergic system to promote their fitness in the intestine.

The gut microbiota regulates several host biochemicals with known neuromodulatory properties, including endocannabinoids, neuropeptides and biogenic amines[6]. Of these, the hormone and neurotransmitter serotonin (5-hydroxytryptamine (5-HT)) is expressed highly in the gastrointestinal tract, synthesized by enterochromaffin cells to levels that account for over 90% of the body's 5-HT content[7]. Approximately 50% of gut-derived 5-HT is regulated by the gut microbiota, particularly spore-forming bacteria dominated by the families _Clostridiaceae_ and _Turicibacteraceae_, with downstream consequences for host intestinal motility, haemostasis and ossification[1-5]. However, whether microbial regulation of host 5-HT occurs as a side effect of bacterial metabolism, or whether there is a functional role for microbial regulation of host 5-HT on bacterial physiology remains unclear. Interestingly, while the majority of gut 5-HT is secreted basolaterally by enterochromaffin cells into surrounding intestinal tissues, some enterochromaffin cell-contained 5-HT is secreted apically into the intestinal lumen[3,5,8],

suggesting that gut microbes are exposed to host-derived 5-HT. Indeed, microbial influences on host enterochromaffin cells regulate 5-HT levels not only in intestinal tissue and blood[1-4], but also in the intestinal lumen and faeces[3,5,8], raising the question of whether there are direct effects of host-derived 5-HT on gut bacteria.

To determine whether the microbiota responds to intestinal 5-HT, we used three approaches to elevate lumenal 5-HT levels and measure their effects on microbiota composition. As a first proof of concept, we supplemented specific pathogen-free (SPF) mice orally with 5-HT to increase faecal 5-HT levels relative to vehicle-treated controls (Fig. 1a). 5-HT substantially enriched species of _Clostridia_ from a combined relative abundance of $10.3 \pm 1.9\%$ (mean ± s.e.m.) in SPF mice to $86.2 \pm 5.8\%$ in 5-HT-supplemented mice (Fig. 1b–d and Supplementary Table 1). This is consistent with previous research showing that spore-forming bacteria dominated by _Clostridiaceae_ and _Turicibacteraceae_ sufficiently promote gut 5-HT[3]. To determine whether physiological increases in host-derived 5-HT similarly alter the gut microbiota, we utilized serotonin transporter (SERT)-deficient mice, which exhibit modest elevations in 5-HT along the intestine[9]. SERT deficiency increased faecal 5-HT by 1.7-fold in SERT^{+/−} mice (Fig. 1e) and enriched _Clostridiaceae_ and _Turicibacter_ from a combined $0.9 \pm 0.3\%$ in wild-type mice to $13.7 \pm 5.5\%$ (Fig. 1f–i and Supplementary Table 2). Notably, these changes were more pronounced in SERT^{+/−} mice, which lack confounding abnormalities in gastrointestinal motility and behaviour compared with SERT^{−/−} mice[10]. To further determine whether genetic predisposition to elevated intestinal 5-HT shapes the gut microbiota, we re-derived the SERT mouse line as germ-free, and inoculated SERT^{+/−} germ-free mice and wild-type germ-free controls with the same SPF faecal microbiota (Supplementary Fig. 1a). At 1 d after inoculation, we observed no overt taxonomic differences; however, at 35 d, SERT^{+/−} mice exhibited significantly increased levels of _Clostridia_, including _Clostridiales_, _Lachnospiraceae_ and _Ruminococcaceae_ (Supplementary Fig. 1b–e and Supplementary Table 3). Overall, these findings reveal that increasing intestinal 5-HT enriches spore-forming bacteria. This supports the notion that induction of host 5-HT by spore-forming bacteria[3] promotes their own community membership in the gut microbiota.

The ability of the microbiota to respond to elevations in host 5-HT suggests that select gut bacteria may encode elements for sensing 5-HT. To evaluate this possibility, we mined bacterial genomes for orthologues of mammalian (human or mouse) SERT. We identified a top candidate with 34% amino acid sequence identity (Supplementary Fig. 2a,b) and predicted structural homology to mammalian SERT (Fig. 2j), which is encoded by all four

[1]Department of Integrative Biology and Physiology, University of California Los Angeles, Los Angeles, CA, USA. [2]Computational Structural Biology Unit, National Institute of Neurological Disorders and Stroke, National Institutes of Health, Bethesda, MD, USA. *e-mail: tcfung@g.ucla.edu; ehsiao@g.ucla.edu
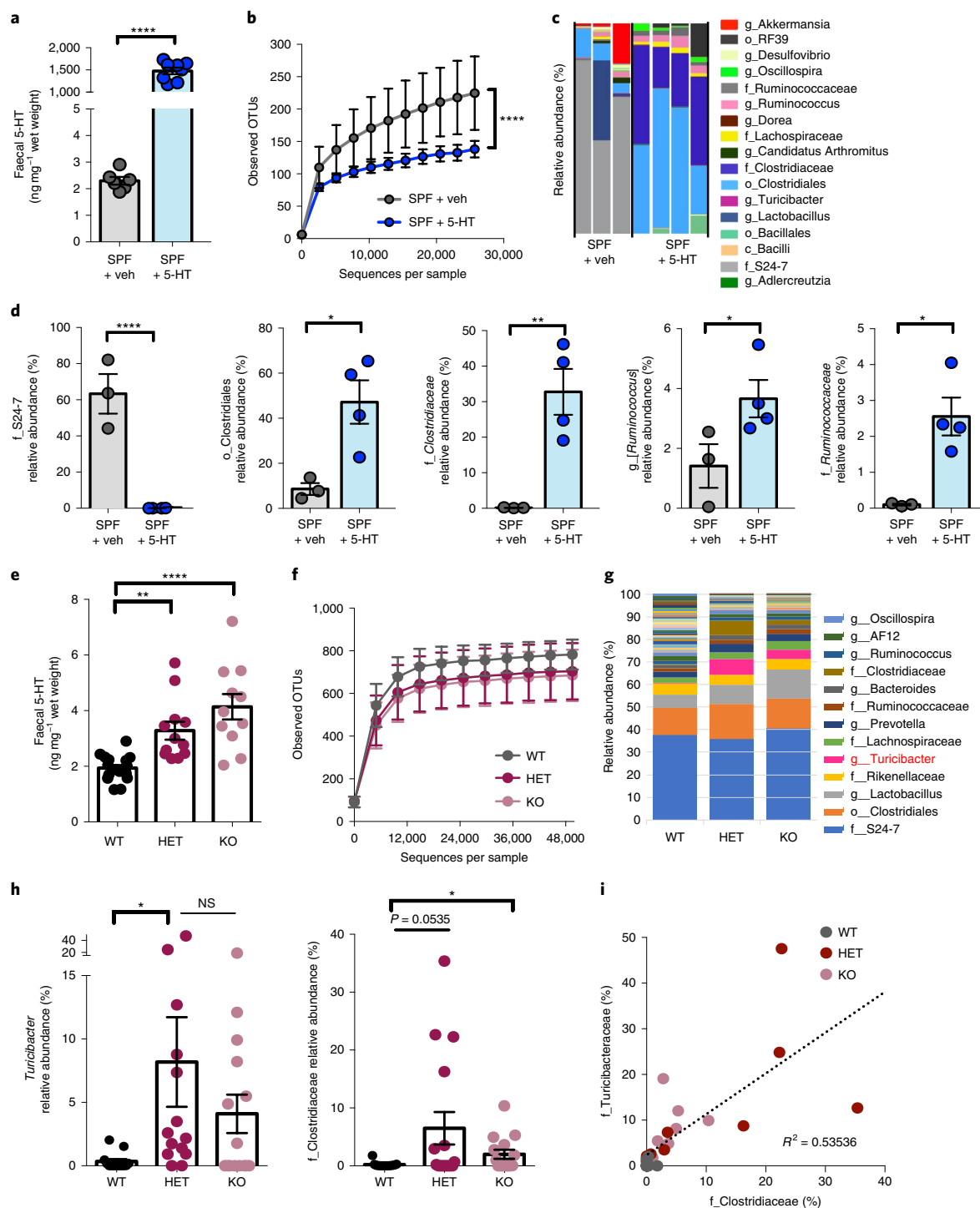
Fig. 1 | Elevating intestinal 5-HT enriches spore-forming bacteria in the gut. a, Faecal 5-HT levels from SPF mice orally supplemented with 5-HT or vehicle in drinking water (two-tailed, unpaired Student's t-test; $n=6$ and 8 cages, respectively). **b**, Alpha diversity of OTUs derived from 16S rDNA sequencing of faeces following vehicle versus 5-HT treatment (two-way ANOVA with Bonferroni test; $n=3$ and 4 cages, respectively). **c**, Taxonomic diversity of the faecal microbiota after vehicle versus 5-HT treatment ($n=3$ and 4 cages, respectively). **d**, Relative abundance of bacterial taxa in faecal microbiota after vehicle versus 5-HT treatment (two-way ANOVA with Kruskal–Wallis test; $n=3$ and 4 cages, respectively). **e**, Faecal 5-HT levels from SPF wild-type (WT), SERT$^{+/-}$ (HET) and SERT$^{-/-}$ (KO) mice (one-way ANOVA with Bonferroni test; $n=13$–15 cages). **f**, Alpha diversity of OTUs derived from 16S rDNA sequencing of faeces from SERT-deficient mice relative to WT controls ($n=10$–12 cages). **g**, Taxonomic diversity of the faecal microbiota after vehicle versus 5-HT treatment. Red font highlights *Turicibacter* in particular ($n=10$–12 cages). **h**, Relative abundance of bacterial taxa in faecal microbiota of SERT-deficient mice relative to WT controls (one-way ANOVA with Kruskal Wallis test; $n=10$, 11 and 12 cages, respectively; $P=0.2134$ for the comparison that is not significant (NS)). **i**, Linear correlation between the relative abundances of *Turicibacteraceae* and *Clostridiaceae* in faecal microbiota from SERT-deficient mice versus WT controls. $R^2=$ coefficient of determination ($n=13$, 15 and 14 cages, respectively). Data are presented as means ± s.e.m. *$P<0.05$; **$P<0.01$; ****$P<0.0001$ (see Supplementary Data Tables 1 and 2 for taxonomic details; see Supplementary Table 11 for detailed statistical information). g, genus; f, family; o, order; c, class.

sequenced strains of the filamentous gut bacterium *Turicibacter sanguinis* and other *Turicibacter* species (Supplementary Table 4). The gene is annotated for *T. sanguinis* HGF1 as a 'putative sodium-dependent 5-HT transporter', and has greater homology to SERT than to LeuT—a promiscuous bacterial amino acid transporter used to model eukaryotic neurotransmitter sodium symporter (NSS) proteins (Supplementary Fig. 2a). Interestingly, *Turicibacter* was enriched particularly in SERT^{+/−} mice, which exhibited increased lumenal bioavailability of 5-HT (Fig. 1g,h). Moreover, *Turicibacter* was the most abundant member of the spore-forming bacterial consortium previously shown to induce host 5-HT biosynthesis[3] (Fig. 2a–c and Supplementary Table 5), and correlated with intestinal 5-HT levels (Fig. 2d,e).

We generated a model of the *Turicibacter* protein based on available structures of human SERT. Given the level of amino acid sequence identity (>30%) between the template and the target sequence, the expected accuracy of this model is 0.7–2.0 Å for the backbone of the transmembrane regions[11]. Indeed, the model scores very highly, consistent with the *Turicibacter* protein being globally similar to human SERT (hSERT) (Supplementary Fig. 3a–e). Residues contributing to the 5-HT and selective 5-HT reuptake inhibitor (SSRI) binding sites in mammalian SERT[12] are strongly conserved (~50% identical and ~70% similar), and the residues required to bind an Na^{+} ion at the so-called Na2 site are identical. However, there were differences in key residues that mediate Cl^{−} dependence (N368, replaced by D262) and neutralization of charged amines (D98, replaced by G22) in mammalian SERT[13,14]. The latter, in particular, raises the question of whether the bacterial orthologue is capable of transporting 5-HT. However, the concurrent substitution of N368 in hSERT by an acidic side chain (D262) just 7 Å away raises the possibility that D262 can play a similar role to D98, allowing for a slightly altered arrangement for 5-HT or inhibitors in a similar binding region.

To determine whether *Turicibacter* is able to detect, import or metabolize 5-HT, we examined the ability of *T. sanguinis* MOL361 to: (1) consume 5-HT in culture; (2) import 4-(4-(dimethylamino)phenyl)-1-methylpyridinium (APP[+]), a molecular substrate for SERT[15]; (3) take up radiolabelled 5-HT; and (4) respond transcriptionally to 5-HT. Culturing *T. sanguinis* in nutrient-rich broth decreased 5-HT levels in the media over time (Fig. 2f). This was prevented by supplementation with the SSRI fluoxetine—a reversible inhibitor of SERT (Fig. 2f) that exhibited cytostatic effects over long-term culture (Supplementary Fig. 4) but not short-term exposure (Fig. 3h and Supplementary Discussion). Exposing *T. sanguinis* to APP[+] resulted in import, which was partially decreased by bacterial pretreatment with unlabelled 5-HT or fluoxetine (Fig. 2g,h). There was also a modest, but not statistically significant, effect of norepinephrine, but not dopamine, on decreasing APP[+] uptake in the assay (Supplementary Fig. 5a). Moreover, *T. sanguinis* imported tritiated 5-HT ([3H] 5-HT), which was inhibited by fluoxetine (Fig. 2i). Notably, fluoxetine had no effect on bacterial uptake of norepinephrine (Supplementary Fig. 5b), suggesting some selectivity to the inhibition of 5-HT import.

Inhibition of 5-HT uptake was not observed by treatment with reserpine or tetrabenazine—inhibitors of mammalian vesicular monoamine transporter (Supplementary Fig. 5c)—suggesting that import of 5-HT by *T. sanguinis* is mediated by an NSS-like protein such as the SERT orthologue (Fig. 2j) rather than a protein in the major facilitator superfamily, such as vesicular monoamine transporter.

To gain insight into whether 5-HT uptake by *T. sanguinis* is mediated by the candidate protein, we cloned the gene from *T. sanguinis* MOL361 ('CUW_0748', as annotated for *T. sanguinis* PC909) into the intestinal bacterium *Bacteroides thetaiotaomicron*, which shows no evidence of endogenous APP[+] import (Supplementary Fig. 6a). Heterologous expression of CUW_0748 in

B. thetaiotaomicron (Supplementary Fig. 6b,c) conferred uptake of APP[+] and 1 μM [3H] 5-HT, which was inhibited by unlabelled 5-HT (Fig. 2k,l). CUW_0748 in *B. thetaiotaomicron* exhibited time-dependent saturation of [3H] 5-HT import (Supplementary Fig. 6d), requiring longer durations than those reported for SERT expressed in mammalian systems[16,17]. Notably, however, CUW_0748 in *B. thetaiotaomicron* failed to show dose-dependent saturation of [3H] 5-HT import; biological variation increased substantially with concentrations of [3H] 5-HT higher than the physiological range (>100 μM) (Supplementary Fig. 6e), which may have been due to stress to *B. thetaiotaomicron*. This indicates that additional studies are needed to validate active transporter-mediated 5-HT import. Notably, there was no effect of CUW_0748 expression on the uptake of tryptophan (Supplementary Fig. 6f), suggesting that it does not function as a tryptophan transporter or broadly disrupt bacterial membrane integrity. These findings suggest that CUW_0748 contributes to 5-HT uptake in *T. sanguinis*, but also leave open the possibility that additional mechanisms for 5-HT import exist. Moreover, it is unclear whether the SERT orthologue, or any unknown 5-HT response elements in *Turicibacter*, are specific to 5-HT as opposed to other biogenic amines, indole derivatives or amino acids. While more research is required to detail the structural and biochemical properties of CUW_0748, these findings demonstrate that *T. sanguinis* imports 5-HT at physiological levels, which is inhibited by fluoxetine, suggesting that transport through an NSS-like protein mediates bacterial 5-HT uptake.

To identify the effects of 5-HT and fluoxetine on bacterial physiology, we profiled transcriptomes of *T. sanguinis* after acute exposure to vehicle, 5-HT, fluoxetine or 5-HT with fluoxetine. 5-HT significantly altered the bacterial expression of 71 genes (Fig. 3a,b), suggesting that *T. sanguinis* responds functionally to 5-HT. Co-treatment of 5-HT with fluoxetine significantly altered 51 of the 71 genes that were differentially expressed in response to 5-HT alone, with additional changes in 344 genes, revealing substantial effects of fluoxetine on bacterial gene expression (Fig. 3a,b and Supplementary Table 6). In particular, 5-HT downregulated the expression of genes that clustered into pathways for cell differentiation, morphogenesis and sporulation (Fig. 3c), and encoded proteins related to efflux transporters, ABC transporters and sporulation (Fig. 3d). Compared with 5-HT-treated controls, fluoxetine upregulated the expression of genes encoding proteins relevant to efflux transporters, ABC transporters and sporulation (Fig. 3e), as well as energy metabolism, metal homeostasis and stress response, suggesting that fluoxetine prevents and/or reverses a subset of 5-HT-mediated changes in *T. sanguinis* gene expression. Consistent with fluoxetine-associated increases in the expression of sporulation-related genes, imaging of *T. sanguinis* exposed to 5-HT with fluoxetine revealed punctate staining of the membrane dye FM 4-64 (Fig. 3f,g)—a phenotype observed during spore formation[18]. Notably, fluoxetine treatment in the absence of 5-HT yielded little change in *T. sanguinis* gene expression (Supplementary Tables 6 and 7), indicating that 5-HT is required for fluoxetine-induced alterations in gene expression. In addition, *T. sanguinis* survival was not affected by acute treatment with 5-HT and/or fluoxetine (Fig. 3h), suggesting that gene expression changes were not due to altered bacterial viability. Overall, these data demonstrate that 5-HT directly alters *T. sanguinis* physiology to reduce the expression of genes related to sporulation and membrane transport, which is abrogated by fluoxetine.

Sporulation is an important determinant of microbial colonization and transmission[19]. Given that 5-HT and fluoxetine regulate the expression of sporulation-related genes in *T. sanguinis*, we tested whether 5-HT and fluoxetine modulate *T. sanguinis* fitness in the intestine. *T. sanguinis* pretreated with vehicle, 5-HT or 5-HT with fluoxetine was orally gavaged into antibiotic-treated SPF mice supplemented with the same chemical treatments in
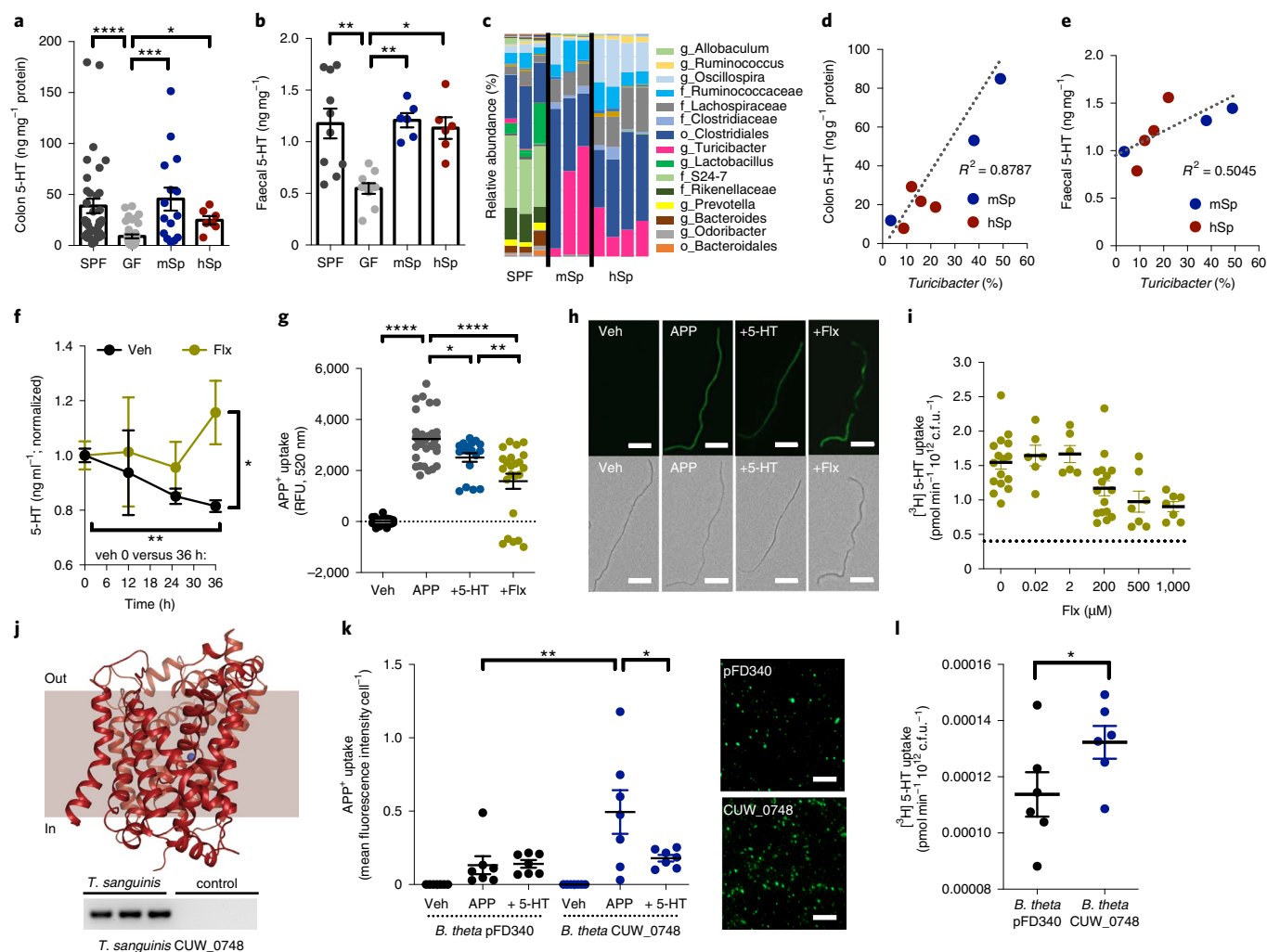
Fig. 2 | *T. sanguinis* takes up 5-HT, which is inhibited by the SSRI fluoxetine. a,b, Colon (**a**) and faecal (**b**) levels of 5-HT in mice that were conventionally colonized (SPF), germ-free (GF) or colonized with mouse-derived (m) or human-derived (h) spore-forming bacteria (Sp) (one-way ANOVA with Bonferroni; $n = 36, 37, 15$ and 7 mice, respectively, in **a**; $n = 10, 10, 6$ and 6 mice, respectively, in **b**). **c**, Taxonomic diversity of the faecal microbiota of SPF, mSp- and hSp-colonized mice ($n = 3, 3$ and 4 cages, respectively). g, genus; f, family; o, order; c, class. **d**, Linear correlation between faecal *Turicibacter* and colon 5-HT ($n = 3$ and 4 cages, respectively). **e**, Linear correlation between faecal *Turicibacter* and faecal 5-HT ($n = 3$ and 4 cages, respectively). **f**, 5-HT in the supernatant after 0, 12, 25 and 36 h of *T. sanguinis* MOL361 growth in Schaedler Broth supplemented with vehicle or 200 μM fluoxetine (two-way ANOVA with Bonferroni test; $n = 3$ and 4 cultures, respectively). **g**, Uptake by *T. sanguinis* exposed to vehicle (veh) or APP[+], either alone (APP) or with 200 μM 5-HT (+5-HT) or fluoxetine (+Flx) pretreatment for 30 min (one-way ANOVA with Bonferroni; test $n = 33, 33, 18$ and 23 cultures, respectively). **h**, Representative images of *T. sanguinis* exposed to veh, APP, +5-HT or +Flx for 30 min (representing $n = 33, 33, 18$ and 23 cultures, respectively). Scale bars, 20 μm. **i**, [³H] 5-HT uptake by *T. sanguinis* at 20 min after pretreatment with veh or +Flx. The dotted line represents the average background signal in negative controls (one-way ANOVA with Bonferroni test; $n = 6$–16 cultures). **j**, Top: predicted structural model for the putative SERT orthologue CUW_0748 in *T. sanguinis* MOL361. Bottom: qPCR product for CUW_0748 cDNA generated from *T. sanguinis* RNA ($n = 3$ cultures). **k**, Left: APP[+] uptake in *B. theta* expressing CUW_0748 or vector controls (pFD340) at 4 h after exposure to veh, APP or +5-HT (one-way ANOVA with Bonferroni test; $n = 7$ cultures). Right: representative images of APP[+] uptake in *B. theta* expressing CUW_0748 or pFD340 controls, with the brightness at 90% higher than that in **h**. Scale bars, 20 μm. **l**, Uptake of 1 μM [³H] 5-HT by *B. theta* expressing CUW_0748 or pFD340 after 20 min (two-tailed unpaired Student's *t*-test; $n = 6$ cultures) Data are presented as means ± s.e.m. *$P < 0.05$; **$P < 0.01$; ***$P < 0.001$; ****$P < 0.0001$ (see Supplementary Data Table 5 for taxonomic details; see Supplementary Table 11 for detailed statistical information).

drinking water. Both vehicle and 5-HT treatment resulted in detectable *T. sanguinis* colonization (Fig. 3i–k). However, treatment with 5-HT and fluoxetine significantly reduced *T. sanguinis* levels in the small intestine (Fig. 3i–k and Supplementary Discussion) and colon (Supplementary Fig. 7a,b), suggesting that fluoxetine-mediated inhibition of 5-HT uptake impairs *T. sanguinis* colonization. Reductions in *T. sanguinis* were similarly seen without additional chemical supplementation in the drinking water, where pretreatment of *T. sanguinis* with 5-HT alone promoted its competitive

colonization in antibiotic-treated mice (Supplementary Fig. 8a–d). In contrast, this effect was not seen with host supplementation alone (Supplementary Fig. 9a,b), suggesting that 5-HT and fluoxetine act directly on *T. sanguinis* to modulate intestinal colonization. Moreover, there was no effect of 5-HT and fluoxetine on *T. sanguinis* in monocolonized mice (Supplementary Fig. 10a,b), suggesting that 5-HT and fluoxetine do not affect the stability of *T. sanguinis* that has already colonized the intestine. In addition, there was no effect of 5-HT and fluoxetine on bacterial colonization of germ-free
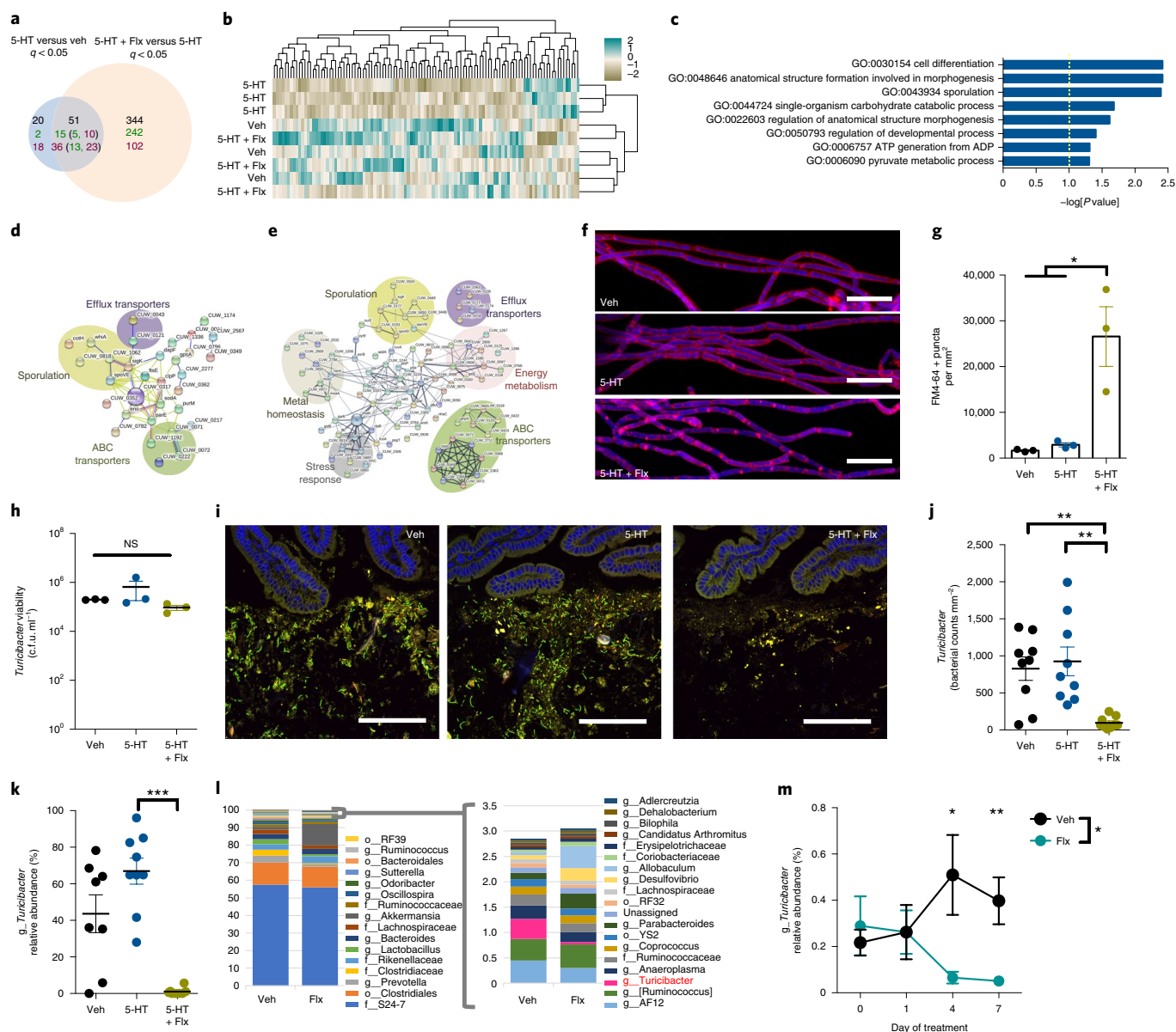
Fig. 3 | 5-HT and the SSRI fluoxetine regulate gene expression and intestinal colonization of *T. sanguinis*. a, Differentially expressed genes (*q* < 0.05) in *T. sanguinis* MOL361 after 4 h exposure to vehicle, 200 μM 5-HT or 5-HT + Flx (black, total genes; green, upregulated genes; red, downregulated genes). Numbers in parentheses represent 5-HT-regulated genes that were further differentially expressed by Flx (Benjamini–Hochberg test; *n* = 3 cultures). **b**, Heatmap of genes with a coefficient of variation < 3 (*n* = 3 cultures). **c**, Gene Ontology (GO) term enrichment analysis of genes differentially expressed in 5-HT versus vehicle and 5-HT + Flx versus 5-HT (Fisher's exact test; *n* = 3 cultures). ADP, adenosine diphosphate; ATP, adenosine triphosphate. **d**, Protein network analysis of 54 genes downregulated in *T. sanguinis* treated with 5-HT versus vehicle (*n* = 3 cultures). **e**, Protein network analysis of 257 genes upregulated in *T. sanguinis* treated with 5-HT + Flx versus 5-HT (*n* = 3 cultures). **f**, Representative images of *T. sanguinis* treated for 24 h with vehicle, 200 μM 5-HT or 5-HT with Flx, and stained with FM 4-64 membrane dye (pink) and DAPI (blue) (*n* = 3 cultures). Scale bars, 10 μm. **g**, Number of FM 4-64 puncta per area of *T. sanguinis* (one-way ANOVA with Bonferroni test; *n* = 3 cultures). **h**, Viability of *T. sanguinis* after 4 h exposure to vehicle, 200 μM 5-HT or 5-HT with Flx (one-way ANOVA with Bonferroni test; *n* = 3 cultures; *P* = 0.9891 for the NS comparison). **i**, Representative FISH images of *T. sanguinis* (green) and small intestinal epithelial cells (DAPI, blue) from antibiotic-treated mice at 3 d after gavage with *T. sanguinis*, pretreated for 4 h with vehicle, 200 μM 5-HT or 5-HT with Flx (*n* = 9 cages). Scale bars, 100 μm. **j**, *T. sanguinis* cell counts from FISH images (one-way ANOVA with Bonferroni test; *n* = 9 cages). **k**, Relative abundance of *Turicibacter* by 16S rDNA sequencing of small intestinal lumenal contents (one-way ANOVA with Bonferroni test; *n* = 9 cages). **l**, Taxonomic diversity based on 16S rDNA sequencing of faecal microbiota on day 7 of Flx treatment. Red font highlights *Turicibacter* in particular. g, genus; f, family; o, order; c, class. **m**, Relative abundance of *Turicibacter* in faeces from SPF mice at 0, 1, 4 and 7 d after gavage with 10 mg kg⁻¹ Flx (two-way ANOVA with Bonferroni test; *n* = 8 and 18 cages, respectively). Data represent means ± s.e.m.; *P* < 0.05; **P* < 0.01; ***P* < 0.001 (see Supplementary Table 11 for detailed statistical information).

mice (Supplementary Fig. 11a,b), suggesting that 5-HT sensing by *T. sanguinis* is important for its competitive colonization within complex microbial communities, and that fluoxetine is not broadly

antimicrobial to *T. sanguinis* under these conditions. Consistent with this, SPF mice gavaged with fluoxetine exhibited decreased *Turicibacter* (Fig. 3l,m) and *Clostridiaceae*, with no significant
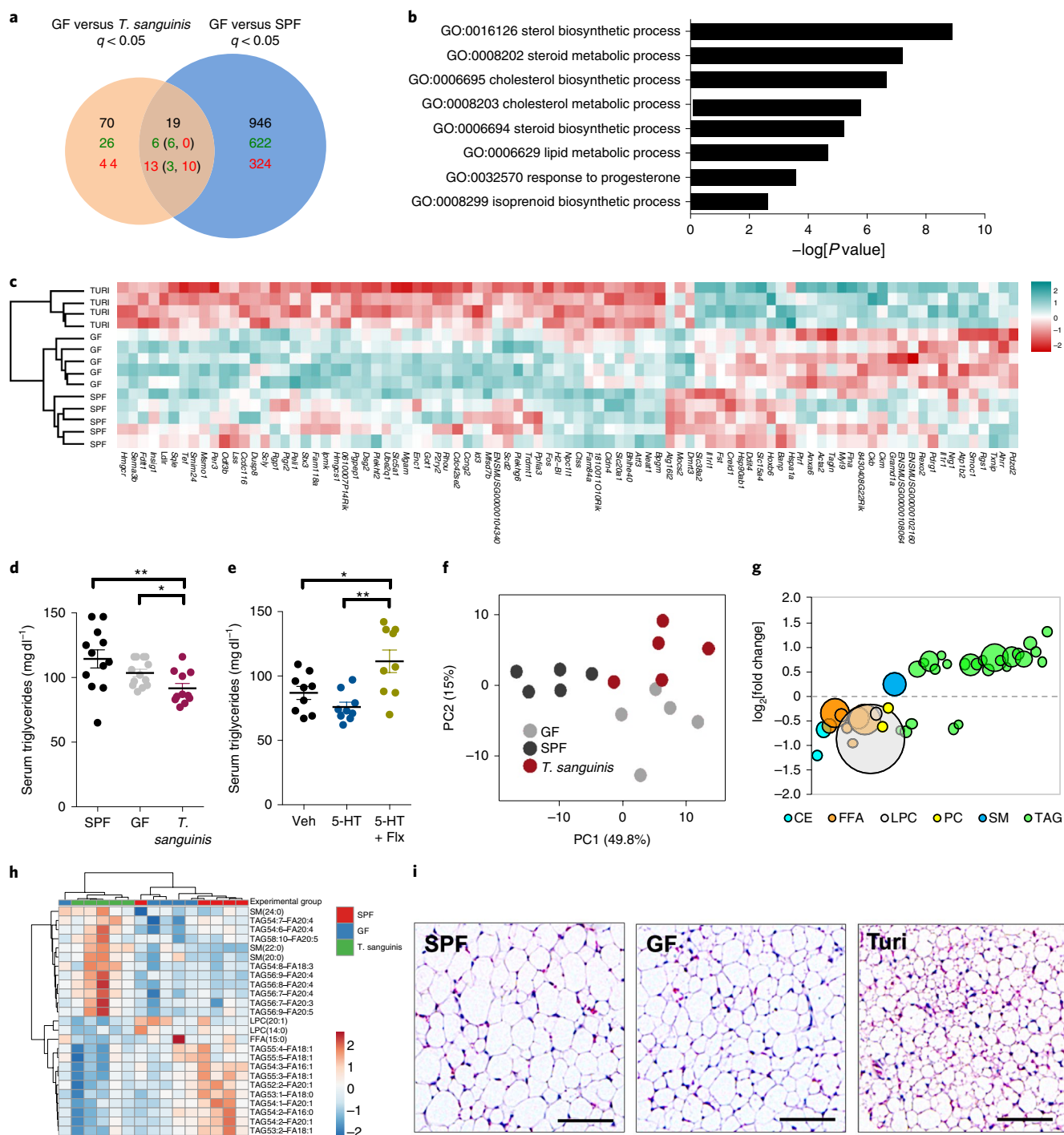
Fig. 4 | _T. sanguinis_ colonization regulates host lipid metabolism. a, Differentially expressed genes ($q < 0.05$) in small intestines from _T. sanguinis_-monocolonized, GF or SPF mice (black, total differentially expressed genes; green, upregulated genes; red, downregulated genes). Numbers in parentheses denote subsets of _T. sanguinis_ regulated genes that were further differentially expressed by SPF (Wald test; $n = 5$, 5 and 4 mice, respectively). **b**, GO term enrichment analysis of genes differentially expressed in the small intestine in response to _T. sanguinis_ relative to GF controls (Fisher's exact test; $n = 4$, 5 and 5 mice, respectively). **c**, Heatmap of the 89 differentially expressed genes in the small intestine in response to _T. sanguinis_ colonization ($n = 5$, 5 and 4 mice, respectively). **d**, Total serum triglyceride levels in GF, SPF and _T. sanguinis_-monocolonized mice (one-way ANOVA with Bonferroni test; $n = 12$, 13 and 11 mice). **e**, Total serum triglyceride levels from antibiotic-treated mice gavaged with _T. sanguinis_ pretreated for 4 h with vehicle, 200 μM 5-HT or 200 μM 5-HT + Flx (one-way ANOVA with Bonferroni test; $n = 9$ mice). **f**, Principal components analysis of plasma lipidomic data for lipid species with $P < 0.05$ for _T. sanguinis_ versus GF and _T. sanguinis_ versus SPF mice (two-way ANOVA with Bonferroni test; $n = 5$ mice). **g**, Average fold change of plasma lipid species ($P < 0.05$) differentially regulated by _T. sanguinis_ compared with GF controls (largest circle, $P < 0.001$; smallest circle, $P < 0.05$). CE, cholesterol esters; FFA, free fatty acids; LPC, lysophosphatidylcholines; PC, phosphatidylcholines; SM, sphingomyelins; TAG, triacylglycerides (two-way ANOVA plus Bonferroni test; $n = 5$ mice). **h**, Heatmap of 25 plasma lipid species similarly increased (red) or decreased (blue) by _T. sanguinis_ colonization relative to both GF and SPF controls ($n = 5$ mice). **i**, Representative image of inguinal white adipose tissue from GF, SPF and _T. sanguinis_-monocolonized mice. Scale bars, 100 μm (representing $n = 5$ mice). Data are presented as means ± s.e.m. *$P < 0.05$; **$P < 0.01$ (see Supplementary Table 11 for detailed statistical information).

differences in bacterial alpha diversity (Supplementary Fig. 12a–c). Collectively, these results suggest that inhibiting bacterial uptake of 5-HT and altering bacterial gene expression by fluoxetine limits the ability of *Turicibacter* to competitively colonize the intestine.

Changes in *Turicibacter* levels have been correlated with particular disease states[20]; however, causal effects of *Turicibacter* on the host remain unknown. To determine how *Turicibacter* colonization impacts host physiology, we first examined intestinal transcriptomes from *T. sanguinis*-monocolonized mice relative to germ-free mice and SPF controls. *T. sanguinis* differentially regulated 89 genes in the small intestine (Fig. 4a and Supplementary Table 8) and 87 genes in the colon (Supplementary Fig. 13a and Supplementary Table 9), which were enriched in pathways for steroid and lipid metabolism (for example, *Hmgcs1*, *Insig1*, *Fift1*, *Msmo1*, *Hmgcr* and *Npc1l1*) (Fig. 4b,c and Supplementary Fig. 13b–c). This was not likely due to bacterial colonization in general, as there was little overlap between the effects of *T. sanguinis* versus SPF colonization on intestinal gene expression (Fig. 4a,b and Supplementary Figs. 13a,b and 14a,b). Moreover, *T. sanguinis*-induced transcriptomic changes were distinct from those reported in mice monocolonized with other species of gut bacteria[21]. In addition to altering the intestinal expression of genes related to lipid metabolism, *T. sanguinis* also reduced host serum triglyceride levels (Fig. 4d). Consistent with this, fluoxetine-induced decreases in *T. sanguinis* were associated with increased serum triglyceride levels compared with mice colonized with vehicle-treated *T. sanguinis* (Fig. 4e). There was no effect of *T. sanguinis* on total serum cholesterol, free fatty acid, low-density lipoprotein or high-density lipoprotein levels (Supplementary Fig. 15). To determine whether *T. sanguinis* modulates concentrations of specific lipid species, we profiled plasma for 1,100 lipids spanning cholesterol esters, ceramides, diacylglycerides, free fatty acids, hexosyl ceramides, lysophosphatidylcholines, lysophosphatidylethanolamines, phosphatidylcholines, sphingomyelins and triacylglycerides (Fig. 4f–h, Supplementary Fig. 16 and Supplementary Table 10). Principal components analysis yielded clustering of lipidomic profiles from *T. sanguinis*-monocolonized mice distinctly from SPF and germ-free controls (Supplementary Fig. 16a and Fig. 4f). A total of 184 lipids were significantly altered by *T. sanguinis* (Supplementary Fig. 16b and Supplementary Table 10), including several triacylglycerides (Fig. 4g and Supplementary Fig. 16c). In particular, *T. sanguinis* reduced levels of long-chain triglycerides containing 18:1 and 20:1 fatty acids, such as oleate and gadoleate, while increasing levels of long-chain triglycerides containing 20:4 and 20:5 polyunsaturated fatty acids, such as arachidonate and eicosapentaenoate (Fig. 4h). The reductions in monoenoic triacylglycerides were consistent with transcriptomic results wherein *T. sanguinis* downregulated the expression of stearoyl-coenzyme A desaturase 2 (*Scd2*) (Fig. 4c)—a rate-limiting enzyme for oleate synthesis[22]. Consistent with reductions in triglyceride levels (Fig. 4d,e), *T. sanguinis*-colonized mice exhibited small multilocular adipocytes in inguinal white adipose tissue (Fig. 4i and Supplementary Fig. 17) and reduced the mass of inguinal white adipose tissue in female, but not male, mice (Supplementary Fig. 18), suggesting that *T. sanguinis* regulates fat mass in a sex-specific manner. These results reveal that *T. sanguinis* modulates host lipid metabolism, and further suggest that regulation of *T. sanguinis* colonization by 5-HT and fluoxetine could have downstream consequences on host physiology (Supplementary Fig. 19).

Considerable progress has been made in understanding host–microbial interactions that control intestinal colonization of select microbial species such as *Bacteroides*[23], but little is known about the molecular determinants of microbial colonization and community membership for other groups of bacteria, including those belonging to the dominant phylum *Firmicutes*. In addition, previous studies on bacterial responses to norepinephrine fuelled the concept of 'microbial endocrinology'[24], but whether host–microbial interactions

occur via other canonical neurotransmitters remains poorly understood. Here, we identify a role for host-derived 5-HT and fluoxetine treatment in regulating the gut microbiota, including intestinal colonization of the gut bacterium *T. sanguinis*. Based on our findings, we propose that particular bacteria indigenous to the gut microbiota, including *Turicibacter*, have co-evolved to induce host 5-HT[1,3,5,8] and further sense host-derived 5-HT to promote their competitive colonization in the intestine. We hypothesize that additional members of the gut microbiota, including particular *Clostridia*, may respond to 5-HT directly through as-yet uncharacterized 5-HT response elements or indirectly through other bacteria, such as *Turicibacter*. Findings from our study support the notion that bidirectional host–microbial signalling via the serotonergic system shapes bacterial communities within the gastrointestinal tract. Notably, a recent human study of >2,700 twins concluded that SSRI use is associated particularly with reduced *Turicibacteraceae* in humans[25], which is consistent with findings from our in silico, in vitro and in vivo animal experiments. These findings, along with increasing associations of *Turicibacter* species with altered immune and metabolic conditions[26–28], raise the question of whether *Turicibacter* impacts host health and disease. Supporting this, we find that monocolonization with *T. sanguinis* alters intestinal lipid metabolism, systemic triglyceride profiles and white adipose tissue physiology in mice, which could be relevant to reported links between SSRI use and symptoms of metabolic syndrome[29,30]. Future studies are needed to investigate the cellular mechanisms by which 5-HT and fluoxetine regulate *T. sanguinis* colonization in the gut and whether fluoxetine-induced changes in the gut microbiota mediate any effects of the SSRI on host intestinal function, neurophysiology and behaviour.

Methods

Mice. C57Bl/6 and SERT−/− mice were purchased from Jackson Laboratories, reared as SPF or C-section re-derived as germ free, and bred in flexible film isolators at the University of California, Los Angeles (UCLA) Center for Health Sciences barrier facility. Breeding animals were fed 'breeder' chow (LabDiet 5K52). Experimental animals were fed standard chow (LabDiet 5010). Colonization status was monitored weekly by aerobic and anaerobic bacterial colony-forming unit (c.f.u.) plating and by 16S ribosomal DNA (rDNA) quantitative PCR (qPCR) from faecal DNA extracted and amplified using the Mo Bio PowerSoil Kit, SYBR Green Master Mix (Thermo Fisher Scientific) and QuantStudio 5 thermocycler (Thermo Fisher Scientific). Mice (6–12 weeks old) were randomly assigned to experimental groups, which included age- and sex-matched cohorts of males and females. Sample sizes for the animal experiments were determined based on previous experience with the experimental paradigm, existing literature utilizing the experimental paradigm, or power calculation. All experiments were performed in accordance with the NIH Guide for the Care and Use of Laboratory Animals using protocols approved by the Institutional Animal Care and Use Committee at UCLA.

5-HT supplementation in mice for microbiota profiling. Water was supplemented with 5-HT (Sigma–Aldrich) at 1.5 mg ml−1 based on calculations from ref. [31] and provided ad libitum to mice for 2 weeks. The amount of water consumed and mouse weight were measured on days 3, 7, 10 and 14 of treatment. Mice were sacrificed 1 d after treatment for 5-HT assays, and faecal 16S rDNA profiling was conducted as described below.

5-HT measurements. Blood samples were collected by cardiac puncture and spun through SST vacutainers (Becton Dickinson) for serum separation. The entire length of the colon or 1-cm regions of the distal, medial and proximal small intestine was washed in phosphate buffered saline (PBS) to remove the luminal contents, and sonicated on ice in 10-s intervals at 20 mV in enzyme-linked immunosorbent assay (ELISA) standard buffer supplemented with ascorbic acid (Eagle Biosciences). Faecal pellets and intestinal contents were weighed and homogenized at 50 mg ml−1 in ELISA standard buffer supplemented with ascorbic acid. Serotonin levels were detected by ELISA according to the manufacturer's instructions (Eagle Biosciences). Readings from tissue samples were normalized to total protein content as detected by bicinchoninic acid assay or the 660 nm Protein Assay (Thermo Pierce).

16S rDNA sequencing. Bacterial genomic DNA was extracted from mouse faecal samples using the Mo Bio PowerSoil Kit. The library was generated according to methods adapted from ref. [32]. The V4 regions of the 16S rDNA gene were PCR amplified using individually barcoded universal primers and 30 ng of the extracted

genomic DNA. The PCR reaction was set up in triplicate, and the PCR product was purified using the QIAquick PCR Purification Kit (Qiagen). In total, 250 ng of purified PCR product from each sample was pooled and sequenced by Laragen using the Illumina MiSeq platform and 2×250-bp reagent kit for paired-end sequencing. Operational taxonomic units (OTUs) were chosen by open reference OTU picking based on 97% sequence similarity to the Greengenes 13_5 database. Taxonomy assignment and rarefaction were performed using QIIME 1.8.0 (ref. [33]). Metagenomes were inferred from closed-reference OTU tables using PICRUSt[34].

Sequence alignment and structural modelling. The Joint Genome Institute Integrated Microbial Genomes and Microbiomes and National Center for Biotechnology Information microbial genomes databases were searched for proteins with sequence similarity to human SERT. Phylogenetic trees were generated for the 15 bacterial candidates with the highest alignment scores using MAFFT[35] and Phylo.io[36]. Primer sets were generated against the SERT homologue ZP_06621923.1 (deprecated to CUW_0748) from *T. sanguinis* PC909 and used to sequence the homologous gene encoding in *T. sanguinis* MOL361, whose product we also named CUW_0748. Protein structural models were created in Phyre2 (ref. [37]) and with MODELLER 9v15 (ref. [38]), based on the highest-resolution available structure of human SERT—namely, Protein Data Bank[39] entry 5i6x chain A, an outward-open conformation bound to paroxetine at 3.14-Å resolution. After initially aligning their sequences using AlignMe version 1.1 in PST mode[40], and inspection of the Ramachandran plot of the initial model, the alignment was refined at positions with strained backbone dihedral angles (see Supplementary Fig. 3a for final alignment), and the model was rebuilt. Based on analysis of the binding site conservation in the initial model, an Na$^+$ ion was included at the Na2 site, using the position observed in a related hSERT template structure (Protein Data Bank entry 5i71 chain A). A total of 500 models were built using different seeds, and a single model was selected—specifically that with the highest ProQM[41] score and fewest Ramachandran outliers—according to PROCHECK[42]. To remove local clashes and optimize geometry, this model was energy minimized using with the CHARMM36 force field[43] with NAMD version 2.9 (ref. [44]), while constraining the backbone atoms and ion at Na2. Further quality assessment was carried out using MolProbity[45] and ConSurf[46] (Supplementary Fig. 3b,e). Structural models were visualized in Chimera[47] and PyMol version 1.7 (Schrödinger). Residues involved in 5-HT, Cl$^-$ and Na$^+$ binding in mammalian SERT were assessed based on the existing literature[13,14,48]. The model is provided in Supplementary Database 1.

Bacterial isolation and cultivation. *T. sanguinis* MOL361 (DSM-14220; DSMZ) was grown in Schaedler Broth (BD Biosciences) in an anaerobic chamber of 5% hydrogen, 10% carbon dioxide and balanced nitrogen. *B. thetaiotaomicron* (ATCC 29148) was grown in Brain Heart Infusion media (BD Biosciences) supplemented with 5 µg ml^{-1} hemin (Frontier Scientific) and 0.5 µg ml^{-1} vitamin K1 (Sigma–Aldrich) under the same anaerobic conditions. Mouse- and human-derived spore-forming bacterial consortia were isolated by chloroform treatment and propagated in mice as described in ref. [3].

Heterologous expression in *B. theta*. CUW_0748 from *T. sanguinis* MOL361 was PCR amplified and cloned into the expression vector pFD340 using the one-step sequence- and ligation-independent cloning protocols described in ref. [49]. The vector was transformed into *E. coli* with selection using 100 µg ml^{-1} ampicillin and conjugated into *B. theta* using the *E. coli* helper plasmid RK231 with 50 µg ml^{-1} kanamycin selection. *E. coli* was killed using 200 µg ml^{-1} gentamicin, and transconjugant strains were selected using 5 µg ml^{-1} erythromycin. Successful conjugation and gene expression were confirmed by PCR and qPCR for CUW_0748 in DNA and RNA extracted from *B. theta* clones.

Turicibacter colonization of germ-free mice. *T. sanguinis* MOL361 was anaerobically cultured as described above. Germ-free mice were colonized by gavage with 200 µl bacterial suspension, or co-housing with dirty bedding from previously colonized mice, and maintained under sterile conditions for at least 2 weeks.

APP$^+$ uptake assay. *T. sanguinis* and *B. theta* were cultured anaerobically as described above and subcultured for 15–17 h to reach the stationary phase. Bacterial APP$^+$ transport activity was measured according to the manufacturer's instructions using the Neurotransmitter Transporter Uptake Assay Kit (Molecular Devices). Briefly, cells were pretreated with vehicle, unlabelled 5-HT (Sigma–Aldrich), fluoxetine (Tocris), dopamine (Sigma–Aldrich) or norepinephrine (Sigma–Aldrich) for 30 min at 37 °C. Dosages were determined based on physiologically and pharmacologically relevant concentrations of ~170 µM 5-HT in the mouse colon[3] and ~130 µM fluoxetine scaled from human clinical treatments[50], respectively. Then, cells were treated with APP$^+$ for 4 h at 37 °C. The intracellular fluorescence signal was measured at 520 nm using a multimodal plate reader (BioTek Synergy H1). Bacterial suspensions were mounted on slides and imaged using an epifluorescence microscope (EVOS). Images of *B. theta* were brightened by 90% to resolve the fluorescence signal.

[^{3}H] 5-HT, [^{3}H] norepinephrine and [^{3}H] tryptophan uptake assays. *T. sanguinis* or *B. theta* were cultured anaerobically as described above and subcultured for 15–17 h to reach the stationary phase. Cells were washed and resuspended in Kreb–Ringer's buffer, then left untreated or pretreated with vehicle, unlabelled 5-HT (Sigma–Aldrich), fluoxetine (Santa Cruz), reserpine (Sigma–Aldrich) or tetrabenazine (Sigma–Aldrich) for 30 min at 37 °C. Cells were then incubated with 1 µM tritiated 5-HT (plus 0–400 µM unlabelled 5-HT for dose-dependent assays), norepinephrine or tryptophan (PerkinElmer). For *T. sanguinis*, all uptake reactions were performed at room temperature. For *B. theta*, uptake reactions were performed at either room temperature or 37 °C.

Uptake reactions were terminated by washing in ice-cold Kreb–Ringer's buffer. Washed *T. sanguinis* was trapped through 0.45-µm polyvinylidene difluoride (PVDF) filters on MultiScreenHTS plates connected to a vacuum manifold (EMD Millipore). For *B. theta*, washed cells were either trapped through 0.45-µm PVDF filters or lysed by incubating in TE buffer plus triton and lysozyme. Extracted filters or lysed cells were incubated in 4 ml Filter Count scintillation fluid (PerkinElmer) for 1 h at room temperature and radioactivity was measured using a liquid scintillation counter (Beckman LS6500).

Bacterial transcriptomic analysis. *T. sanguinis* was cultured anaerobically as described above and subcultured to the stationary phase. Cells were incubated in culture media supplemented with vehicle, 200 µM 5-HT (Sigma–Aldrich), fluoxetine (Tocris) or 5-HT with fluoxetine for 4 h at 37 °C. Bacteria were washed with PBS and lysed in TE buffer containing 1.2% Triton X-100 and 15 mg ml^{-1} lysozyme. RNA was extracted using the RNAeasy Mini Kit with on-column genomic DNA-digest (Qiagen). Complementary DNA (cDNA) synthesis was performed using the qScript cDNA Synthesis Kit (Quantabio). RNA quality of RNA integrity number > 8.0 was confirmed using the 4200 Tapestation system (Agilent). Ribosomal RNA was removed with the Ribo-Zero Bacteria Kit (Illumina). RNA was prepared using the TruSeq Stranded RNA Kit (Illumina), and 2×75-bp paired-end reads were sequenced using the Illumina HiSeq platform by the UCLA Neuroscience Genomics Core. The bacterial RNA sequencing analysis package Rockhopper[51] was used for quality filtering, mapping against the *T. sanguinis* PC909 genome and differential expression analysis. Over 23.79 million reads were obtained for each sample, with 86–88% aligning to protein-coding genes. Heatmaps containing differentially expressed genes with an adjusted $P < 0.05$ and a coefficient of variation (s.d./mean) < 3 were generated using the pheatmap package for R. Gene Ontology term enrichment analysis of differentially expressed genes with adjusted $P < 0.05$ was conducted using DAVID[52]. Functional protein networks were generated with differentially expressed genes with adjusted $P < 0.05$ using STRING[53].

Bacterial FM 4-64 staining and imaging. Overnight cultures of *T. sanguinis* MOL361 were pooled and treated with vehicle, 5-HT (200 µM), fluoxetine (200 µM) or 5-HT and fluoxetine (both 200 µM) for 24 h at 37 °C. Cells were washed with PBS, fixed in 4% paraformaldehyde, and stained with FM4-64 (5 µg ml^{-1}) and 4′,6-diamidino-2-phenylindole (DAPI; 0.2 µg ml^{-1}) according to the manufacturer's instructions. Cells were wet-mounted on glass slides and cover slips. Images were acquired at 63× using the Zeiss LSM 780 confocal microscope. Images were analysed using Fiji software[54] by a researcher blinded to the experimental group. FM 4-64 puncta were counted manually based on circularity and fluorescence intensity. Counts were normalized to cell area, as determined by thresholding of DAPI staining.

Turicibacter colonization of antibiotic-treated mice. SPF mice were treated with ampicillin, gentamicin, neomycin and vancomycin in their drinking water at 0.5 g l^{-1} for 4 d. Faecal samples were collected and plated anaerobically to confirm bacterial clearance. After an additional day on sterile water, antibiotic-treated mice were orally gavaged once daily for 5 d with 10^6 c.f.u. mouse^{-1} *T. sanguinis* MOL361 that was pretreated with 200 µM 5-HT, fluoxetine or vehicle for 4 h at 37 °C. Mice were also maintained on regular water, 5-HT (24 µg ml^{-1}) or 5-HT (24 µg ml^{-1}) with fluoxetine (40 µg ml^{-1}) in the drinking water over the same 5 d of *Turicibacter* oral gavage. The fluoxetine drinking water concentration was determined so that each mouse would receive an effective dose of 10 mg kg^{-1} d^{-1}. The 5-HT drinking water concentration was determined by calculating the same molar concentration as Flx in the drinking water. This dose of 5-HT elevated faecal levels by approximately sixfold over vehicle. Three days after the final gavage, mice were euthanized by CO$_2$ and the small and large intestines were collected for fluorescence in situ hybridization (FISH) as described below. Lumenal contents from the small and large intestines were harvested for 16S rDNA sequencing. In the 'drinking-water-only' experimental approach, mice were gavaged with untreated *T. sanguinis* once daily for 5 d and maintained on regular water, 5-HT or 5-HT with fluoxetine in the drinking water. Tissues were collected and analysed 3 d after the final gavage. In the 'bacterial pretreatment only' experimental approach, mice were gavaged with one or three doses of vehicle, 5-HT or 5-HT with fluoxetine-pretreated *T. sanguinis* once daily and sacrificed 12–24 h after the final gavage.

Bacterial FISH. Mouse intestines were fixed in Carnoy's fixative overnight at 4 °C, washed and transferred to 70% ethanol. Intestinal samples were then paraffin embedded and cut into 5-µm longitudinal sections by IDEXX Bioresearch.

Slides were deparaffinized with xylene, rehydrated in ethanol and incubated in 1 µM FISH probe (Sigma–Aldrich) in hybridization buffer (0.9 M NaCl, 20 mM Tris-HCl (pH 7.2) and 0.1% sodium dodecyl sulfate) for 4 h at 50 °C in a humidified chamber. The *Turicibacter* probe TUR176 was used: 5′ [6FAM]-GCAYCTTTAAACTTTCGTCCTATCCG. Slides were then washed three times in preheated wash buffer (0.9 M NaCl and 20 mM Tris-HCl (pH 7.2)) and mounted with ProLong Gold Antifade Mountant with DAPI (Invitrogen). Images were acquired on a Zeiss LSM 780 confocal microscope at 20× magnification. Image analyses were performed using ImageJ.

Fluoxetine treatment for 16S rDNA sequencing. SPF mice were orally gavaged daily for 7 d with 10 mg kg^{-1} fluoxetine (Santa Cruz) or treated with fluoxetine (40 µg ml^{-1}) in the drinking water for 14 d as indicated in the figure captions. Faecal samples were harvested on day 0, 1, 4, 7 or 14 of treatment, as indicated in figure captions, and processed for 16S rDNA sequencing as described above.

Intestinal transcriptomic analysis. Sections of the terminal ileum and distal colon (1 cm) were harvested from SPF, germ-free or *Turicibacter*-monocolonized mice, washed with PBS to remove the lumenal contents, and homogenized using 5-mm stainless steel beads (Qiagen) for 1 min in a Mini-Beadbeater-16 (BioSpec Products). RNA was extracted using the RNAeasy Mini Kit with on-column genomic DNA digest (Qiagen), and cDNA synthesis was performed using the qScript cDNA Synthesis Kit (Quantabio). RNA quality of RNA integrity number > 8.9 was confirmed using the 4200 Tapestation system (Agilent). RNA was prepared using the QuantSeq mRNA-Seq Library Prep Kit (Lexogen), and 1 × 65-bp 3′ reads were sequenced using the Illumina HiSeq platform by the UCLA Neuroscience Genomics Core. The BlueBee analysis platform (Lexogen) was used for quality filtering and mapping. Differential expression analysis was conducted using DESeq2 (ref. [55]). At least 8.47 million aligned reads were obtained for each sample. Heatmaps containing differentially expressed genes with $q < 0.05$ were generated using the pheatmap package for R. Gene Ontology term enrichment analysis of differentially expressed genes with $q < 0.05$ was conducted using DAVID[52].

Lipid clinical chemistry analysis. Serum samples were collected from SPF, germ-free, *Turicibacter*-monocolonized or *Turicibacter*-enriched mice and submitted to Charles River Clinical Pathology for analysis of the lipid species, including total cholesterol, free fatty acids, high-density lipoprotein, low-density lipoprotein and total triglycerides.

Plasma lipidomic analysis. Lipids from 25 µl of plasma were extracted using a modified Bligh and Dyer extraction method by the UCLA lipidomics core facility[56]. Before biphasic extraction, a 13-lipid class Lipidyzer Internal Standard Mix was added to each sample (5040156; AB Sciex). Following two successive extractions, pooled organic layers were dried down in a Genevac EZ-2 Elite evaporator. Lipid samples were resuspended in 1:1 methanol/dichloromethane with 10 mM ammonium acetate and transferred to robovials (10800107; Thermo Fisher Scientific) for analysis[56]. Samples were analysed on the Sciex Lipidyzer Platform for targeted quantitative measurement of 1,100 lipid species across 13 classes. The Differential Mobility device on the Lipidyzer was tuned with a SelexION Tuning Kit (5040141; Sciex). Instrument settings, tuning settings and the multiple reaction monitoring (MRM) list are available on request.

Adipocyte histology and imaging. Epididymal, gonadal and inguinal white adipose tissues were collected from SPF, germ-free and *Turicibacter*-monocolonized mice. Tissues were weighed, fixed in 4% paraformaldehyde for 48 h, transferred to 70% ethanol and submitted to IDEXX Pathology Services for paraffin sectioning and embedding. Sections of 5 µm were stained with haematoxylin and eosin and imaged at 20× magnification.

Adipocyte cell morphologies and numbers were quantified using ImageJ.

Statistical methods. All statistical data are included in Supplementary Table 11. Statistical analysis was performed using Prism software (GraphPad). Data were plotted in the figures as means ± s.e.m. For each figure, n = the number of independent biological replicates. Differences between two treatment groups were assessed using two-tailed, unpaired Student's t-tests with Welch's correction. Differences among more than two groups with only one variable were assessed using one-way ANOVA with Bonferroni post-hoc test. Taxonomic comparisons from 16S rDNA sequencing analysis were analysed by Kruskal–Wallis test with Bonferroni post-hoc test. Two-way ANOVA with Bonferroni post-hoc test was used for two or more groups with two variables. Significant differences emerging from the above tests are indicated in the figures by *$P < 0.05$, **$P < 0.01$, ***$P < 0.001$ and ****$P < 0.0001$ Notable near-significant differences ($0.5 < P < 0.1$) are also indicated in the figures. Notable non-significant (and non-near-significant) differences are indicated in the figures by 'NS'.

Reporting Summary. Further information on research design is available in the Nature Research Reporting Summary linked to this article.

Data availability

Data generated or analysed during this study are included in this published article and its Supplementary Information files. Structural modelling files that support the findings of this study are available from Zenodo with the identifier 10.5281/zenodo.3266444. The 16S rDNA sequencing data that support the findings of this study are available from the Qiita database with study IDs 12585, 12596 and 12597, and are also available in the Supplementary Tables. Bacterial transcriptomic data that support the findings of this study are available in Gene Expression Omnibus repository with the accession number GSE133810 and are also available in the Supplementary Tables. Intestinal transcriptomic data that support the findings of this study are available in the Gene Expression Omnibus repository with the accession number GSE133809 and are also available in the Supplementary Tables.

References

1. Vuong, H. E., Yano, J. M., Fung, T. C. & Hsiao, E. Y. The microbiome and host behavior. *Annu. Rev. Neurosci.* **40**, 21–49 (2017).
2. Gershon, M. D. & Tack, J. The serotonin signaling system: from basic understanding to drug development for functional GI disorders. *Gastroenterology* **132**, 397–414 (2007).
3. Reigstad, C. S. et al. Gut microbes promote colonic serotonin production through an effect of short-chain fatty acids on enterochromaffin cells. *FASEB J.* **29**, 1395–1403 (2015).
4. Wikoff, W. R. et al. Metabolomics analysis reveals large effects of gut microflora on mammalian blood metabolites. *PLoS ONE* **106**, 3698–3703 (2009).
5. Yano, J. M. et al. Indigenous bacteria from the gut microbiota regulate host serotonin biosynthesis. *Cell* **161**, 264–276 (2015).
6. Sjogren, K. et al. The gut microbiota regulates bone mass in mice. *J. Bone Min. Res.* **27**, 1357–1367 (2012).
7. Hata, T. et al. Regulation of gut luminal serotonin by commensal microbiota in mice. *PLoS ONE* **12**, e0180745 (2017).
8. Fujimiya, M., Okumiya, K. & Kuwahara, A. Immunoelectron microscopic study of the luminal release of serotonin from rat enterochromaffin cells induced by high intraluminal pressure. *Histochem. Cell Biol.* **108**, 105–113 (1997).
9. Mawe, G. M. & Hoffman, J. M. Serotonin signalling in the gut—functions, dysfunctions and therapeutic targets. *Nat. Rev. Gastroenterol. Hepatol.* **10**, 473–486 (2013).
10. Chen, J. J. et al. Maintenance of serotonin in the intestinal mucosa and ganglia of mice that lack the high-affinity serotonin transporter: abnormal intestinal motility and the expression of cation transporters. *J. Neurosci.* **21**, 6348–6361 (2001).
11. Olivella, M., Gonzalez, A., Pardo, L. & Deupi, X. Relation between sequence and structure in membrane proteins. *Bioinformatics* **29**, 1589–1592 (2013).
12. Coleman, J. A. & Gouaux, E. Structural basis for recognition of diverse antidepressants by the human serotonin transporter. *Nat. Struct. Mol. Biol.* **25**, 170–175 (2018).
13. Forrest, L. R., Tavoulari, S., Zhang, Y. W., Rudnick, G. & Honig, B. Identification of a chloride ion binding site in Na$^+$/Cl$^-$-dependent transporters. *Proc. Natl Acad. Sci. USA* **104**, 12761–12766 (2007).
14. Barker, E. L., Moore, K. R., Rakhshan, F. & Blakely, R. D. Transmembrane domain I contributes to the permeation pathway for serotonin and ions in the serotonin transporter. *J. Neurosci.* **19**, 4705–4717 (1999).
15. Solis, E. Jr. et al. 4-(4-(dimethylamino)phenyl)-1-methylpyridinium (APP$^+$) is a fluorescent substrate for the human serotonin transporter. *J. Biol. Chem.* **287**, 8852–8863 (2012).
16. Chanrion, B. et al. Physical interaction between the serotonin transporter and neuronal nitric oxide synthase underlies reciprocal modulation of their activity. *Proc. Natl Acad. Sci. USA* **104**, 8119–8124 (2007).
17. Seimandi, M. et al. Calcineurin interacts with the serotonin transporter C-terminus to modulate its plasma membrane expression and serotonin uptake. *J. Neurosci.* **33**, 16189–16199 (2013).
18. Ramijan, K. et al. Stress-induced formation of cell wall-deficient cells in filamentous actinomycetes. *Nat. Commun.* **9**, 5164 (2018).
19. Browne, H. P. et al. Culturing of 'unculturable' human microbiota reveals novel taxa and extensive sporulation. *Nature* **533**, 543–546 (2016).
20. Goodrich, J. K., Davenport, E. R., Waters, J. L., Clark, A. G. & Ley, R. E. Cross-species comparisons of host genetic associations with the microbiome. *Science* **352**, 532–535 (2016).
21. Geva-Zatorsky, N. et al. Mining the human gut microbiota for immunomodulatory molecules. *Cell* **168**, 928–943 (2017).
22. Miyazaki, M., Dobrzyn, A., Elias, P. M. & Ntambi, J. M. Stearoyl-CoA desaturase-2 gene expression is required for lipid synthesis during early skin and liver development. *Proc. Natl Acad. Sci. USA* **102**, 12501–12506 (2005).
23. Porter, N. T., Canales, P., Peterson, D. A. & Martens, E. C. A subset of polysaccharide capsules in the human symbiont *Bacteroides thetaiotaomicron*

promote increased competitive fitness in the mouse gut. *Cell Host Microbe* **22**, 494–506 (2017).

24. Lyte, M., Villageliu, D. N., Crooker, B. A. & Brown, D. R. Symposium review: microbial endocrinology—why the integration of microbes, epithelial cells, and neurochemical signals in the digestive tract matters to ruminant health. *J. Dairy Sci.* **101**, 5619–5628 (2018).

25. Jackson, M. A. et al. Gut microbiota associations with common diseases and prescription medications in a population-based cohort. *Nat. Commun.* **9**, 2655 (2018).

26. Goodrich, J. K. et al. Genetic determinants of the gut microbiome in UK twins. *Cell Host Microbe* **19**, 731–743 (2016).

27. Bernstein, C. N. & Forbes, J. D. Gut microbiome in inflammatory bowel disease and other chronic immune-mediated inflammatory diseases. *Inflamm. Intest. Dis.* **2**, 116–123 (2017).

28. Guo, X. et al. High fat diet alters gut microbiota and the expression of Paneth cell-antimicrobial peptides preceding changes of circulating inflammatory cytokines. *Mediat. Inflamm.* **2017**, 9474896 (2017).

29. Lee, S. H., Paz-Filho, G., Mastronardi, C., Licinio, J. & Wong, M. L. Is increased antidepressant exposure a contributory factor to the obesity pandemic? *Transl. Psychiatry* **6**, e759 (2016).

30. Beyazyuz, M., Albayrak, Y., Egilmez, O. B., Albayrak, N. & Beyazyuz, E. Relationship between SSRIs and metabolic syndrome abnormalities in patients with generalized anxiety disorder: a prospective study. *Psychiatry Invest.* **10**, 148–154 (2013).

31. Abdala-Valencia, H. et al. Inhibition of allergic inflammation by supplementation with 5-hydroxytryptophan. *Am. J. Physiol. Lung Cell Mol. Physiol.* **303**, L642–L660 (2012).

32. Caporaso, J. G. et al. Global patterns of 16S rRNA diversity at a depth of millions of sequences per sample. *Proc. Natl Acad. Sci. USA* **108**, 4516–4522 (2011).

33. Caporaso, J. G. et al. QIIME allows analysis of high-throughput community sequencing data. *Nat. Methods* **7**, 335–336 (2010).

34. Langille, M. G. et al. Predictive functional profiling of microbial communities using 16S rRNA marker gene sequences. *Nat. Biotechnol.* **31**, 814–821 (2013).

35. Katoh, K., Rozewicki, J. & Yamada, K. D. MAFFT online service: multiple sequence alignment, interactive sequence choice and visualization. *Brief Bioinform.* https://doi.org/10.1093/bib/bbx108 (2017).

36. Robinson, O., Dylus, D. & Dessimoz, C. Phylo.io: interactive viewing and comparison of large phylogenetic trees on the web. *Mol. Biol. Evol.* **33**, 2163–2166 (2016).

37. Kelley, L. A., Mezulis, S., Yates, C. M., Wass, M. N. & Sternberg, M. J. The Phyre2 web portal for protein modeling, prediction and analysis. *Nat. Protoc.* **10**, 845–858 (2015).

38. Webb, B. & Sali, A. Comparative protein structure modeling using MODELLER. *Curr. Protoc. Protein Sci.* **86**, 2.9.1–2.9.37 (2016).

39. Berman, H. M. et al. The Protein Data Bank. *Nucleic Acids Res.* **28**, 235–242 (2000).

40. Stamm, M., Staritzbichler, R., Khafizov, K. & Forrest, L. R. AlignMe—a membrane protein sequence alignment web server. *Nucleic Acids Res.* **42**, W246–W251 (2014).

41. Wallner, B. ProQM-resample: improved model quality assessment for membrane proteins by limited conformational sampling. *Bioinformatics* **30**, 2221–2223 (2014).

42. Laskowski, R. A., Rullmannn, J. A., MacArthur, M. W., Kaptein, R. & Thornton, J. M. AQUA and PROCHECK-NMR: programs for checking the quality of protein structures solved by NMR. *J. Biomol. NMR* **8**, 477–486 (1996).

43. Best, R. B. et al. Optimization of the additive CHARMM all-atom protein force field targeting improved sampling of the backbone ϕ, ψ and side-chain χ_1 and χ_2 dihedral angles. *J. Chem. Theory Comput.* **8**, 3257–3273 (2012).

44. Phillips, J. C. et al. Scalable molecular dynamics with NAMD. *J. Comput. Chem.* **26**, 1781–1802 (2005).

45. Williams, C. J. et al. MolProbity: more and better reference data for improved all-atom structure validation. *Protein Sci.* **27**, 293–315 (2018).

46. Ashkenazy, H. et al. ConSurf 2016: an improved methodology to estimate and visualize evolutionary conservation in macromolecules. *Nucleic Acids Res.* **44**, W344–W350 (2016).

47. Pettersen, E. F. et al. UCSF Chimera—a visualization system for exploratory research and analysis. *J. Comput. Chem.* **25**, 1605–1612 (2004).

48. Coleman, J. A., Green, E. M. & Gouaux, E. X-ray structures and mechanism of the human serotonin transporter. *Nature* **532**, 334–339 (2016).

49. Jeong, J. Y. et al. One-step sequence- and ligation-independent cloning as a rapid and versatile cloning method for functional genomics studies. *Appl. Environ. Microbiol.* **78**, 5440–5443 (2012).

50. Hiemke, C. & Hartter, S. Pharmacokinetics of selective serotonin reuptake inhibitors. *Pharm. Ther.* **85**, 11–28 (2000).

51. McClure, R. et al. Computational analysis of bacterial RNA-Seq data. *Nucleic Acids Res.* **41**, e140 (2013).

52. Huang, D. W., Sherman, B. T. & Lempicki, R. A. Systematic and integrative analysis of large gene lists using DAVID bioinformatics resources. *Nat. Protoc.* **4**, 44–57 (2009).

53. Szklarczyk, D. et al. The STRING database in 2017: quality-controlled protein–protein association networks, made broadly accessible. *Nucleic Acids Res.* **45**, D362–D368 (2017).

54. Schindelin, J. et al. Fiji: an open-source platform for biological-image analysis. *Nat. Methods* **9**, 676–682 (2012).

55. Love, M. I., Huber, W. & Anders, S. Moderated estimation of fold change and dispersion for RNA-Seq data with DESeq2. *Genome Biol.* **15**, 550 (2014).

56. Bligh, E. G. & Dyer, W. J. A rapid method of total lipid extraction and purification. *Can. J. Biochem. Physiol.* **37**, 911–917 (1959).

Acknowledgements

Author contributions

T.C.F. performed the bacteriology, sequencing experiments and data analysis. C.D.G.L. and A.V. assisted with the bacteriology experiments. T.C.F., H.E.V. and G.N.P. performed the mouse experiments. A.A.A., N.G.R. and L.R.F. performed the structural modelling. J.M. and T.R. generated the gnotobiotic mice. L.R.F. and E.Y.H. contributed to the data analysis. T.C.F., L.R.F. and E.Y.H. supervised the study. T.C.F. and E.Y.H. wrote the manuscript. All authors reviewed and edited the final version of the text.

Competing interests

Additional information

nature research

Corresponding author(s): Elaine Y. Hsiao

Reporting Summary

Nature Research wishes to improve the reproducibility of the work that we publish. This form provides structure for consistency and transparency in reporting. For further information on Nature Research policies, see Authors & Referees and the Editorial Policy Checklist.

Statistical parameters

When statistical analyses are reported, confirm that the following items are present in the relevant location (e.g. figure legend, table legend, main text, or Methods section).

n/a	Confirmed	
☐	☒	The exact sample size (*n*) for each experimental group/condition, given as a discrete number and unit of measurement
☐	☒	An indication of whether measurements were taken from distinct samples or whether the same sample was measured repeatedly
☐	☒	The statistical test(s) used AND whether they are one- or two-sided *Only common tests should be described solely by name; describe more complex techniques in the Methods section.*
☐	☒	A description of all covariates tested
☐	☒	A description of any assumptions or corrections, such as tests of normality and adjustment for multiple comparisons
☐	☒	A full description of the statistics including central tendency (e.g. means) or other basic estimates (e.g. regression coefficient) AND variation (e.g. standard deviation) or associated estimates of uncertainty (e.g. confidence intervals)
☐	☒	For null hypothesis testing, the test statistic (e.g. F, t, r) with confidence intervals, effect sizes, degrees of freedom and P value noted *Give P values as exact values whenever suitable.*
☒	☐	For Bayesian analysis, information on the choice of priors and Markov chain Monte Carlo settings
☒	☐	For hierarchical and complex designs, identification of the appropriate level for tests and full reporting of outcomes
☒	☐	Estimates of effect sizes (e.g. Cohen's *d*, Pearson's *r*), indicating how they were calculated
☐	☒	Clearly defined error bars *State explicitly what error bars represent (e.g. SD, SE, CI)*

Our web collection on statistics for biologists may be useful.

Software and code

Policy information about availability of computer code

Data collection	Image acquisition: Zeiss ZEN Blue **v2.3** and Black **v2.3SP1** Scintillation counting: Beckman LS6500
Data analysis	Protein sequence alignment and structural modeling: MAFFT **v7**, Phylo.io, Phyre2 **v2**, MODELLER 9v15, AlignMe v1.1 , ProQM, ProCheck, NAMD **v2.9**, CHARMM36, MolProbity **v4.4**, ConSurf, Chimera **v1.13.1**, PyMol v1.7 Bacterial transcriptomic analysis: Rockhopper **v2.0.3**, DAVID **v6.8**, STRING **v11.0** Intestinal transcriptomic analysis: BlueBee **1.10**, DESeq2 **v3.9**, R studio **v1.0.143**, DAVID **v6.8** 16S rDNA sequencing: QIIME1.8.0, PICRUSt **v1** Image analysis: ImageJ **v1.8.0**, Zeiss ZEN Blue **v2.3** and Black **v2.3SP1** Statistical analysis: GraphPad Prism **v8**

For manuscripts utilizing custom algorithms or software that are central to the research but not yet described in published literature, software must be made available to editors/reviewers upon request. We strongly encourage code deposition in a community repository (e.g. GitHub). See the Nature Research guidelines for submitting code & software for further information.

Data

All manuscripts must include a data availability statement. This statement should provide the following information, where applicable:

- Accession codes, unique identifiers, or web links for publicly available datasets
- A list of figures that have associated raw data
- A description of any restrictions on data availability

Data generated or analyzed during this study are included in this published article (and its supplementary information files).

Field-specific reporting

Please select the best fit for your research. If you are not sure, read the appropriate sections before making your selection.

☒ Life sciences ☐ Behavioural & social sciences ☐ Ecological, evolutionary & environmental sciences

For a reference copy of the document with all sections, see nature.com/authors/policies/ReportingSummary-flat.pdf

Life sciences study design

All studies must disclose on these points even when the disclosure is negative.

Sample size	Group size estimates were determined by power calculation and based on previous experience with the model system and experimental paradigm.
Data exclusions	No acquired data were excluded from experiments.
Replication	All experiments were replicated at least 3 times and all attempts were successful.
Randomization	Age- and sex-matched animals were randomly allocated into experimental groups.
Blinding	Investigators were blinded to experimental group where possible: for 16S rDNA sequencing prep and analysis, bacterial transcriptomic sequencing prep and analysis, intestinal transcriptomic sequencing prep and analysis, FISH image analysis, neurotransmitter uptake assay image analysis.

Reporting for specific materials, systems and methods

Materials & experimental systems

n/a	Involved in the study
☐	☒ Unique biological materials
☒	☐ Antibodies
☒	☐ Eukaryotic cell lines
☒	☐ Palaeontology
☐	☒ Animals and other organisms
☒	☐ Human research participants

Methods

n/a	Involved in the study
☒	☐ ChIP-seq
☒	☐ Flow cytometry
☒	☐ MRI-based neuroimaging

Unique biological materials

Policy information about availability of materials

Obtaining unique materials	Turicibacter and B. theta bacterial strains are available from DSMZ culture collection, SERT GF mice are available upon request from the investigators, SERT SPF mice are available through Jackson Laboratory.

Animals and other organisms

Policy information about studies involving animals; ARRIVE guidelines recommended for reporting animal research

Laboratory animals	Mouse C57Bl/6, adult >8 weeks, males and females sex-matched.

| Wild animals | The study did not involve wild animals. |
| Field-collected samples | The study did not involve samples collected from the field. |